2020 IEEE International Conference on Robotics and Automation (ICRA)
31 May - 31 August, 2020. Paris, France

A Shape Memory Polymer Adhesive Gripper For Pick-and-Place Applications

ChangHee Son and Seok Kim, *Member, IEEE*

***Abstract*—Over the past few years, shape memory polymer (SMP) has been extensively studied in terms of its remarkable reversible dry adhesive properties and related smart adhesive applications. However, its exceptional properties have not been exploited for further opportunities such as pick-and-place applications, which would otherwise advance the robotic manipulation. This work explores the use of an SMP to design an adhesive gripper that picks and places a target solid object employing the reversible dry adhesion of an SMP. Compared with other single surface contact grippers including vacuum, electromagnetic, electroadhesion, and gecko grippers, the SMP adhesive gripper interacts with not only flat and smooth dry surfaces but also moderately rough and even wet surfaces for pick-and-place with high adhesion strength (> 2 atmospheres). In this work, associated physical mechanisms, SMP adhesive mechanics, and thermal conditions are studied. In particular, the numerical and experimental study elucidates that the optimal compositional and topological SMP design may substantially enhance its adhesion strength and reversibility, which leads to a strong grip force simultaneously with a minimized releasing force. Finally, the versatility and utility of the SMP adhesive gripper are highlighted through diverse pick-and-place demonstrations.**

I. Introduction

Robotic grippers have highly been explored for numerous applications in diverse fields. The aerospace industry requires gravity-independent or zero-gravity grippers to use in space [1-2]. Electronics companies need pick-and-place robotic grippers to assemble devices using surface mounting technologies [3]. The manufacturing or logistics industry has also a strong demand for grippers to lift heavy objects or to do repetitive manipulations that lessen the burden of human workers [4-6]. Microassembly utilizing grippers have enabled unique 3-dimensional microelectromechanical systems (MEMS) which cannot be achieved using other conventional approaches [7-9].

To satisfy the aforementioned demands, various mechanisms for robotic grippers have been introduced. Finger grippers are simple yet effective when optimized by choosing the number of fingers and the shape of their gripping motions with appropriate actuation methods [10-12]. Soft grippers show favorable performances since they resemble real human fingers [13]. However, both finger and soft grippers have a common drawback that the target objects they lift must have multiple surfaces with acceptable dimensions to be gripped. Using microspine grippers is a great choice to interact with rough surfaces such as rocks [1,14] although they are not capable of working for smooth surfaces inherently. Electromagnetic grippers have a benefit of easy and fast lifting and releasing [15] if lifting objects are made of ferrous materials, which is their intrinsic drawback in terms of material choice. Electroadhesion grippers based on the electrostatic force are also beneficial for quick pick-and-place due to their fast response speed [16]. Nevertheless, their adhesion strength is relatively low unless the voltage is very high, which is prone to damaging electronic parts on adhering surfaces. Vacuum grippers are capable of lifting heavy weight objects and they can also be used for wall-climbing [17-18]. However, they would not work in a vacuum nor for porous surface objects. More recent gecko grippers do not need any atmosphere so that it can be used in space [2] and adhere to surfaces made of any materials [19-20]. Those grippers are promising but their limited adhesion strength, working only for dry surfaces and somewhat complicated manufacturing or operation may suppress their broader adaptation.

In this work, a shape memory polymer (SMP) is employed to design an adhesive gripper which exploits SMP's strong, material-independent, reversible, and dry adhesion to pick and place flat, smooth or moderately rough surface objects. Furthermore, since SMP's dry adhesion is wet-tolerant, the SMP adhesive gripper is working for wet or submerged objects as well [21]. These unique adhesive properties of the SMP adhesive gripper possibly eliminate or mitigate the challenges involved in other existing grippers. An SMP is a class of external stimuli-responsive polymer with the shape memory effect, i.e., the ability to stably fix its deformed or 'temporary' shape and fully recover its original or 'permanent' shape. In particular, a thermoresponsive SMP undergoes a substantial change in storage modulus across the glass transition temperature (T_g) between glassy and rubbery states, and generally shows a strong shape memory effect upon

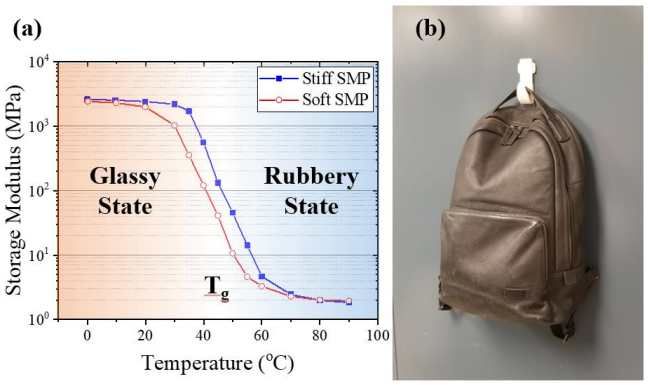

Figure 1 (a) The storage moduli of stiff and soft shape memory polymers (SMPs) as a function of temperature. (b) Application of the SMP for a reversible dry adhesive hook.

C. Son and S. Kim are with the Mechanical Science and Engineering Department, University of Illinois at Urbana-Champaign, Urbana, IL 61801 USA (corresponding author (S. Kim) to provide phone: 217-265-5656; e-mail: skm@ illinois.edu).

thermomechanical loading [21-25]. With applied heat and pressure, an SMP becomes soft in its rubbery state and makes a conformal and hermetic contact with dry or wet opposing surface. After cooled with pressure, the SMP becomes rigid in its glassy state yet maintains its contact with the opposing surface which forms a strong dry adhesion. However, once reheated, the SMP tends to lose its contact and strong adhesion, resulting in the reversible dry adhesion. Fig. 1 depicts the storage moduli of the SMPs used in this work as a function of temperature and their use as an adhesive hook that is recently demonstrated. The storage moduli are measured using TA instrument Q800 Dynamic Mechanical Analysis.

Over the integrated design of an SMP adhesive gripper by combining SMP adhesives and a mechanical releasing mechanism, we also present the mechanics at the adhesive interface upon compositional and topological variations of the SMP adhesive. The analysis of temperature associated with heating and cooling modules of the gripper assists the final design of the SMP adhesive gripper towards its pick-and-place demonstration.

II. Methods

A. Schematics

Fig. 2 shows the computer-aided design (CAD) model and the photograph of the SMP adhesive gripper which has three legs and three feet. Legs and feet are connected using ball joints with maximum swivel angle of 35°. A pin-in-slot joint is used to connect the middle link and both top and bottom links. The body is built primarily with machined aluminum and 3D printed parts. The three feet are all parallelly connected to an 11.1 V, 1200 mAh Lithium Polymer (LiPo) battery (Kinexsis). Wires between feet and the external lead of the gripper are concealed inside aluminum frames. Three Peltier modules are under three feet and utilized for heating/cooling cycles. To control the Peltier modules by switching electrical polarity and thus the direction of current flow, 15 ampere maximum double-pole, double-throw (DPDT) switch with 'center position off' is used.

B. Pick-and-Place Procedure

In the picking step, the SMP is heated up to the rubbery state. Then the preload is applied and the SMP is cooled down to the glassy state simultaneously. At this state, the gripper is attached to the target object and is ready for picking due to the strong dry adhesion of the SMP. In the placing step, similarly, the SMP is heated up to the rubbery state and thus to the weak adhesion state. With the operator's manipulation, a releasing force is applied to peel the SMP. As a result, the gripper is able to place the target object.

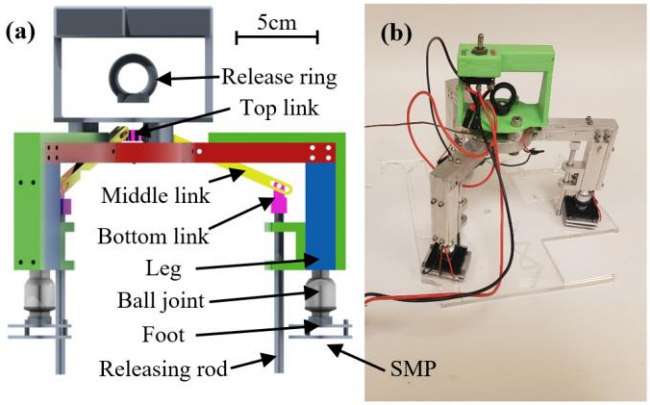

Figure 2 (a) The CAD drawing and (b) the photograph of an SMP adhesive gripper. The gripper has a battery and a thermocouple for heating/cooling and temperature sensing.

C. Fabrication of SMP

The SMP that is used in this work is prepared based on the procedure developed elsewhere [22]. First, Poly(Bisphenol A-co-epichlorohydrin), glycidyl end-capped with a molecular weight of 1075 g/mol from Sigma-Aldrich, hereafter called E1075, and diglycidyl ether of bisphenol A epoxy monomer with a molecular weight of 362 g/mol from Momentive, hereafter called EPON 826, are preheated in a 110 °C oven. When they are completely melted, E1075 and EPON 826 are mixed to make the epoxy monomer. The curing agent Jeffamine D-230 poly(propylene glycol)bis(2-aminopropyl) ether with an average molecular weight of about 230 from Huntsman, hereafter called Jeffamine, is then mixed into the epoxy monomer. The weight-based mixing ratio of E1075 : EPON 826 : Jeffamine is 0.940 : 1.000 : 0.837 for the stiff SMP and 0.334 : 1.000 : 0.707 for the soft SMP. The resulting SMP precursor is poured on a PTFE tape (Tapecase) covered 3 x 2 inch glass slide and air bubbles inside the mixture are removed using a pipette. The curing takes place in a hot oven at 80 °C for 120 minutes. After the SMP is fully cured, it is easily peeled off from the PTFE tape in its glassy state.

Two types of SMP samples are prepared. The first type SMP samples are used to quantitatively evaluate their adhesion strength upon diverse compositional and topological design variations. For a single SMP sample, a cured stiff SMP is cut into a 25 mm diameter round shape using Fusion M2 laser cutter from Epilog Laser (Fig. 3a). The other single SMP can also made of a cured soft SMP in the identical way. For a dual SMP sample, a cured soft SMP is cut into a 5 mm width and 25 mm outer diameter ring shape using the laser cutter. Then a stiff SMP precursor is filled in the center hollow area and cured (Fig. 3b). The completed SMP sample is finally attached to a backing aluminum block using Loctite Instant Mix epoxy. For an SMP sample with release tip, a cured stiff SMP is cut into a 25 mm diameter round shape. Then a single

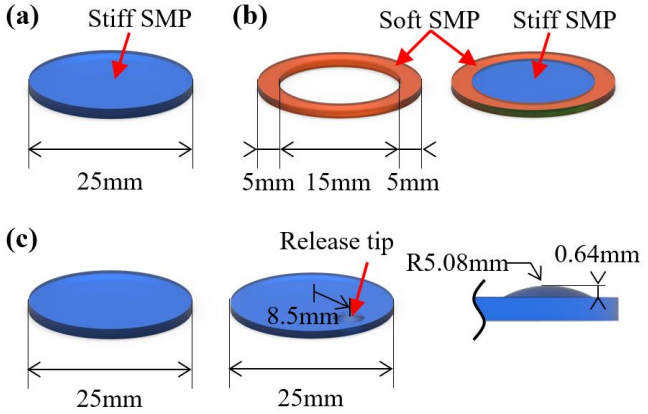

Figure 3 (a) Fabrication of a single SMP sample. A stiff SMP is cured and cut into a 25 mm diameter round shape. (b) Fabrication of a dual SMP sample. A soft SMP is cured and cut into a ring shape and a stiff SMP precursor is subsequently filled and cured inside the ring-shaped soft SMP. (c) Fabrication of an SMP sample with release tip. To form a release tip on a 25 mm diameter SMP sample, a single drop of SMP precursor is placed on the SMP surface and then cured.

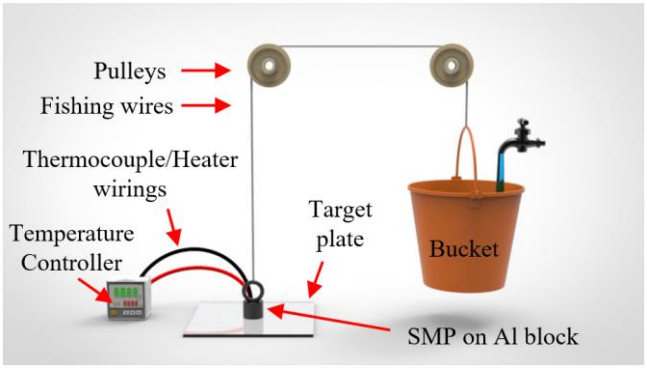

Figure 4 The test setup to measure the adhesion strength of an SMP sample. While an SMP adheres to the target plate, the bucket is filled with water. Once the SMP fails in adhering to the target plate, its adhesion strength is recorded.

drop of stiff SMP precursor is placed on the cured stiff SMP sample using a pipette. As shown in Fig. 3c a release tip is 8.5 mm away from the center and its radius is 5.08 mm with the maximum height of 0.64 mm.

The second type of SMP samples used for the pick-and-place demonstration are made by directly pouring and curing the stiff SMP precursor on aluminum plates. After curing the plates are attached to Peltier modules.

D. Adhesion Test Setup

The test setup to measure the adhesion strength is shown in Fig. 4. The backing aluminum block where an SMP is fixed is connected to a bucket through the pulleys using a fishing wire. The block has a cartridge heater and a thermocouple inside which are connected to a temperature controller. To measure the maximum adhesion of the glassy SMP, the SMP is first heated to approximately 80 ˚C and becomes its rubbery state. Then the preload of 12.67 kg (2.50 atm) is applied on the SMP to achieve conformal adhesive contact with the acrylic target plate. During preloading, the heater is off and the SMP is cooled. After cooling to approximately 30 ˚C, the SMP turns out to be the glassy state and water is slowly pumped into the bucket. To measure the minimum adhesion of the rubbery SMP, the glassy SMP adhering to the acrylic target plate is reheated to approximately 80 ˚C before slowly pumping water into the bucket. The maximum or minimum adhesion strength of the glassy or rubbery SMP is recorded when the SMP fails in adhering to the acrylic target plate by measuring the weight of water and the bucket.

E. Heating and Cooling Modules

While a simple cartridge heater is used to heat the SMP for the adhesion strength test, the final SMP adhesive gripper uses a Peltier module (TEC1-12710) not only to heat but also to actively cool the SMP. Fig. 5 shows the Peltier module between two aluminum plates. The thickness of aluminum plates is chosen to be 2 mm since it is thin enough for the heat to quickly reach the SMP but thick enough to have tap holes.

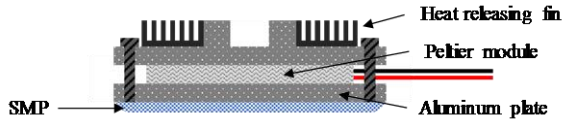

Figure 5 A schematic of a Peltier module assembled with heat releasing fins and aluminum plates.

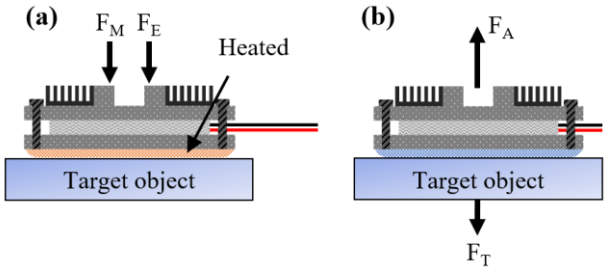

Figure 6 The free body diagram of the foot of an SMP adhesive gripper. (a) Forces during preloading. (b) Forces during picking.

When using the Peltier module, fins are used to release heat such that the whole system does not heat up. Otherwise, the SMP would not be cooled sufficiently.

III. Result and Discussion

A. Picking Mechanism

In the picking step, an SMP is heated and brought down to a target object and ball joints between legs and feet passively rotate to achieve a conformal contact. Fig. 6a shows the step where applying a preload which is the sum of the gripper weight (F_M) and an external force (F_E). Since the preload is critical to adhesive performance [23], it is desirable to have large F_E to meet the below inequality where P_{pre} is the minimum preload pressure to ensure reliable adhesive grip.

$$(F_M + F_E) / A > P_{pre}. \quad (1)$$

After cooling, the SMP adheres to the target object and the gripper is able to pick it up. At this step, the weight of the target object (F_T) should not exceed the adhesive force of the SMP (F_A) as shown in Fig. 6b. The adhesion strength of the SMP to a flat and smooth glass plate (P_S) is 5-30 N/cm^2, which was characterized previously [24].

Therefore, the maximum weight that the gripper can pick up should be,

$$F_T < F_A = P_S \times A. \quad (2)$$

Using the magnitude of A in Table I, F_T should be smaller than 240 N if P_S is assumed to be 5 N/cm^2 and F_T should be smaller than 1440 N if P_S is assumed to be 30 N/cm^2.

TABLE I. Parameters of SMP Adhesive Gripper

Parameter	Symbol	Magnitude
Weight of the device	F_M	12.7 N
Minimum preload pressure	P_{pre}	15 N/cm^2 [23]
Total SMP area	A	48 cm^2
Angle between the middle link and the leg	θ	0-33.6°
Length from pivot point O to top link	L_a	25 mm
Length from pivot point O to bottom link	L_b	50 mm
Release ring pulling force	F_H	60 N [26]

B. Placing Mechanism

Fig. 7a magnifies a pin-in-slot joint previously shown in Fig. 2a, which connects the middle and bottom links. Once the SMP adhesive gripper adheres to a target object, the links do not make any displacement such that a static situation can be

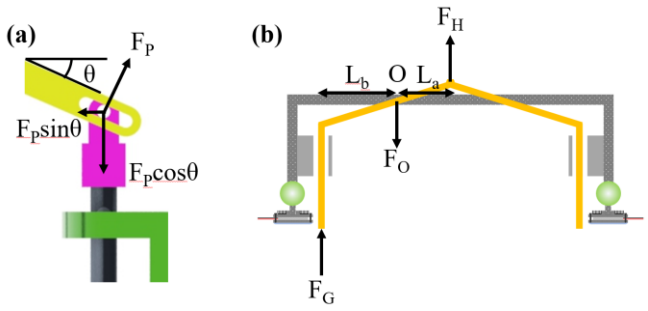

Figure 7 (a) The magnified view of a pin-in-slot joint used between the links. (b) The schematic of the SMP adhesive gripper and the free body diagram of the links.

assumed. In this static situation, the force is applied from the slot to the pin which is labeled as F_P in Fig. 7a. This force can be split into the horizontal and vertical forces which are F_P $sin\theta$ and F_P $cos\theta$, and thus

$$F_P = F_P\, cos\theta + F_P\, sin\theta. \quad (3)$$

Evidently, the vertical force (F_P $cos\theta$) is equal to the reaction force from the ground (F_G) which is labeled in Fig. 7b.

$$F_G = F_P\, cos\theta. \quad (4)$$

For placing the target object, applying a larger F_G is more desirable since the SMP is more easily peeled off from the target object. Using (4), F_G can be maximized by setting the initial angle of the middle link (θ) to be zero.

Fig. 7b shows the forces that are applied to the middle link. Through the middle link, a force applied to the releasing ring is transferred to the releasing rods with mechanical advantage. F_H is the force that is applied to the release ring per each leg in order to peel off the SMP and place the target object. Simultaneously, reaction force (F_G) is applied from the target object. In a static situation, the sum of the moment at the pivot point O should be zero,

$$\Sigma M_O = F_H L_a - F_G L_b = 0. \quad (5)$$

Where L_a and L_b indicate the distance between point O and the bottom or top link. When F_H of 60 N is applied [26], F_G calculated to be 30 N by using (5) together with L_a and L_b in Table I. In addition, for the force equilibrium, the following equation should be met in a static situation of the middle link in Fig. 7b,

$$\Sigma F = F_H + F_G - F_O = 0. \quad (6)$$

Therefore, the force applied to the middle link at point O (F_O) is calculated to be 90 N. Simultaneously, the leg of the gripper receives the same amount of force as F_O but in opposite direction.

C. SMP Adhesion - Simulation

To study the effect of SMP's stiffness and composition on its adhesion, a finite element analysis (FEA) on the first principal stress is conducted. As shown in Fig. 8a, the displacement is constrained at the SMP bottom surface which is in contact with a target plate. The external load is applied to the top of the aluminum block. Assuming that the SMP is in glassy state at 30 °C, Young's modulus is chosen as 2000 MPa for the stiff SMP and 1000 MPa for the soft, which are inferred from the data in Fig. 1a. The resultant first principal stress at the bottom surface of the SMP along the A-A` line is shown. Both stiff and soft single SMP shows extremely high stress concentration at the edge of the SMP. Whereas the dual SMP shows that the stress is more evenly distributed to the center which helps reduce the outer edge stress concentration. As a result of the reduced stress concentration at the outer edge, the contact failure starting at the outer edge occurs with higher external load. This indicates the dual SMP is supposed to exhibit higher maximum adhesion strength than both single SMPs, which is similar to the results shown in the previous study [27].

Further numerical analysis is conducted to compare the minimum adhesion strength of the rubbery SMP with and without release tip. The boundary condition is shown in Fig. 8b. A prescribed displacement of 0.74 mm has been applied downwards to a target plate that does not deform. This value is chosen to completely compress the release tip (0.64 μm thick) and ensure a small amount of additional compression of 0.1 μm to the rest of the SMP. Assuming that the SMP is in

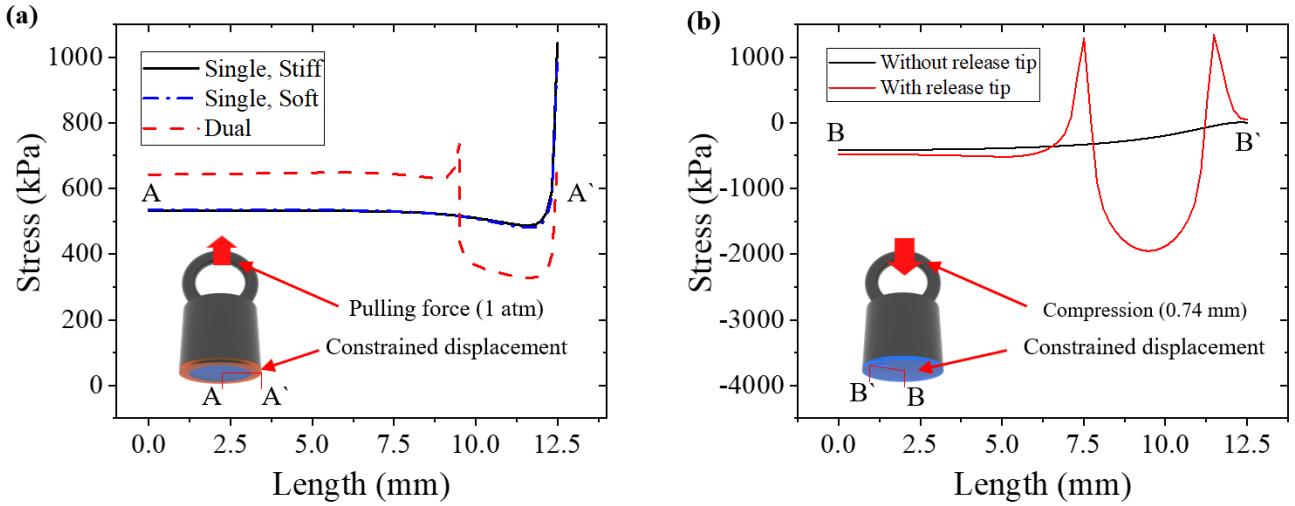

Figure 8 (a) The schematic dual SMP sample attached to the aluminum block with its boundary condition and the plot of the first principal stress along the A-A` line computed using FEA. (b) The schematic SMP with release tip attached to the aluminum block with its boundary condition and the plot of the first principal stress along the B-B` line computed using FEA.

rubbery state at 80 °C, Young's modulus is chosen as 20 MPa. The resultant first principal stress that occurs at the bottom surface of the SMP along the B-B` line is shown. The SMP without release tip only shows the compressive stress which increases towards the center. On the other hand, the SMP with release tip shows dramatical stress concentration near the release tip and shows both tensile and compressive stress. Consequently, if the prescribed displacement is removed in the rubbery state, the SMP with release tip tends to pop up and may show self-peeling due to the high stress concentration near the release tip. However, the glassy state SMP with release tip after the compression does not tend to pop up since the compressed tip shape is fixed. Therefore, adding a release tip to the SMP reduces the minimum adhesion of the rubbery SMP and may enable its self-peeling without significantly compromising its maximum adhesion in the glassy state.

D. SMP Adhesion - Experimental Results

The qualitative prediction of the enhanced adhesion strength and reversibility (the ratio between maximum and minimum adhesion strength) with dual SMP and release tip SMP designs are quantified through the experimental adhesion strength measurement. Fig. 9a shows the maximum adhesion strength of single and dual SMPs measured using the test setup introduced in Fig. 4. After three tests per an individual sample, the average adhesion strength for single soft SMP, single stiff SMP and dual SMP are measured to be 1.75 atm, 2.28 atm, and 4.83 atm respectively. Fig. 8a shows that the stress concentration for both single soft and stiff SMPs are almost identical. However, the soft SMP accumulates more strain energy than the stiff SMP when the same load is applied, which means the soft SMP is more susceptible to contact failure. Therefore, the experimentally measured maximum adhesion strength of the soft SMP is smaller than that of the stiff SMP. More importantly, the maximum adhesion strength of the dual SMP is over twice higher than those of single SMPs. Due to high stress concentration, the edge of the single SMPs is more vulnerable to contact failure. However, as predicted in the simulation, the dual SMP distributes the stress more evenly from edge to center, and therefore the maximum adhesion strength is considerably enhanced.

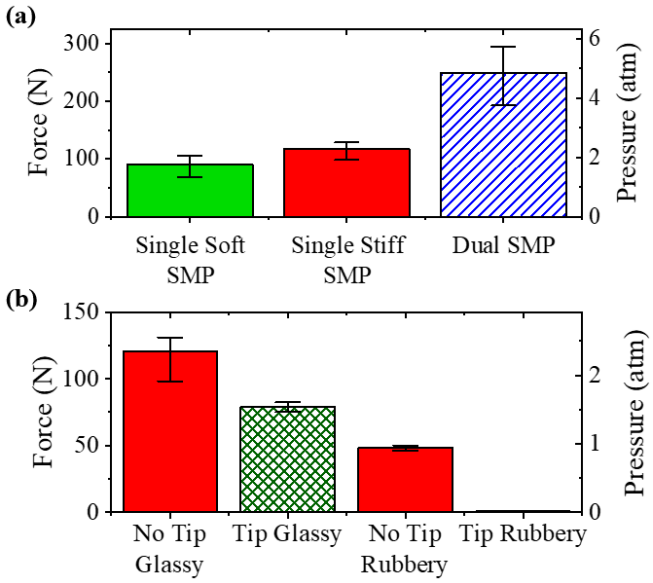

Figure 9 (a) The experimentally measured maximum adhesion strength of single and dual SMPs. (b) The experimentally measured adhesion strength of SMPs with and without release tip in the glassy and rubbery states.

Fig. 9b shows the maximum and minimum adhesion strength of SMPs with and without release tip measured using the same test setup shown in Fig. 4. The results indicate that the maximum adhesion strength of glassy SMPs decreases from 2.35 atm to 1.54 atm once a release tip is added. However, the minimum adhesion strength which is the required force to peel off the SMP in the rubbery state dramatically decreases from 0.936 atm to 0.00955 atm when a release tip is added. Since the peeling force of the rubbery SMP with release tip is almost negligible, it can be regarded as self-peeling. The self-peeling of the SMP should be quite beneficial in real-life applications even though the release tip sacrifices 34 % of the maximum adhesion strength of the glassy SMP. Therefore, adopting the dual SMP with release tip would raise the adhesion strength and reversibility of the SMP more efficiently since it increases the maximum adhesion strength while in the glassy state but decreases the peeling force while in the rubbery state.

E. Temperature Analysis

A thermocouple is utilized to characterize the temperature profile of the SMP adhesive gripper foot that is heated and cooled with a Peltier module powered by fully charged 3 cell LiPo battery. In Fig. 10, the SMP side indicates the temperature of the SMP and the Fin side indicates the temperature of the heat releasing fin. For the first 30 seconds, heat flows from the fin side to the SMP side since the heating switch is on. After 20 second heating, the SMP temperature is raised over 80 °C. Between 36 second and 52 second the cooling switch is on so that the current flows in the opposite direction. In this condition, the heat flows from the SMP side to the fin side, which remarkably reduces the cooling time compared to the natural convection cooling. Immediately after the cooling switch is off, the SMP side temperature becomes about 40 °C. However, due to residual heat in the fin side, the final temperature of the SMP side is raised up again to 48 °C and slowly decreases. It is worthwhile to note that high adhesion of the SMP is still achieved even slight above T_g like 40-50 °C since the SMP actually passes through a glass transition temperature range, not a sharp transition at T_g, which is inferred from Fig. 1.

F. Demonstration

To demonstrate the pick-and-place of the SMP adhesive

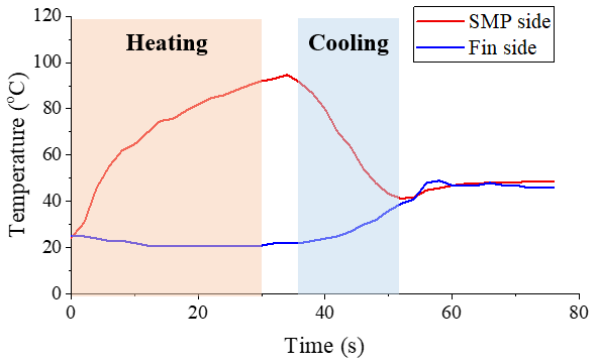

Figure 10 The temperature profile of an SMP adhesive gripper foot during heating and cooling with a Peltier module as a function of time.

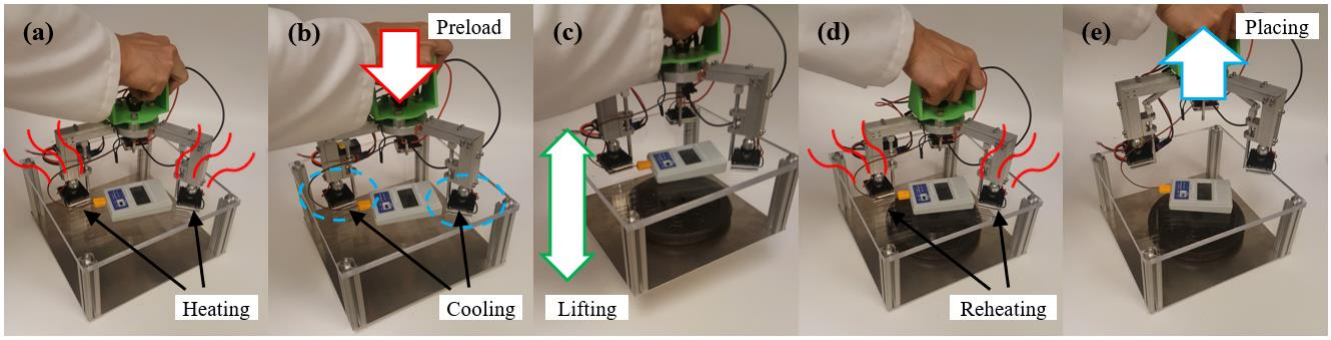

Figure 11 The pick-and-place demonstration of the SMP adhesive gripper.

gripper operated with one hand, a 30 cm × 30 cm × 14 cm stage with an acrylic plate top is built. Fig. 11a-b show the picking step where the SMP is heated over 90 °C, then preloaded and at the same time cooled down to 40 °C. A mass of 4.5 kg is added to the stage and the SMP adhesive gripper picks up this weight as shown in Fig. 11c. Finally, Fig. 11d-e show that the SMP is reheated over 90 °C and a releasing force is applied to place the weight.

The SMP in this work is capable of adhering not only to dry, flat and smooth surfaces but also to wet, non-flat or moderately rough surfaces. Fig. 12 demonstrates that the SMP adhesive gripper picks up surfaces with various roughness, an angled surface, and a wet surface. These results show a highly positive prospect on the use of the SMP adhesive gripper in a practical situation. The optical images and the surface roughness profiles of sandpaper, wood, tile, poster paper and acrylic plate surfaces used in the demonstration are obtained using Keyence VK-X1000 3D laser scanning confocal microscope as shown in Fig. 13. Based on these surface profile data, the arithmetic average roughness (R_a) magnitudes of the surfaces are 14.1 µm (sandpaper), 6.58 µm (wood), 0.267 µm (tile), 2.04 µm (poster paper), and 0.983 µm (acrylic plate), respectively.

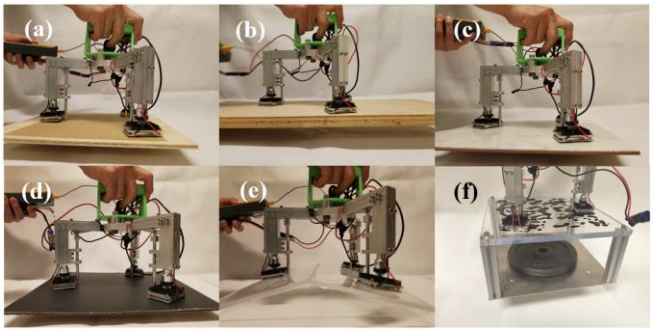

Figure 12 The images of the SMP adhesive gripper picking various surfaces including (a) a sandpaper, (b) a wooden plate, (c) a tile, (d) a poster paper, (e) and an angled acrylic plate, and (f) an acrylic plate wet with blue dyed water.

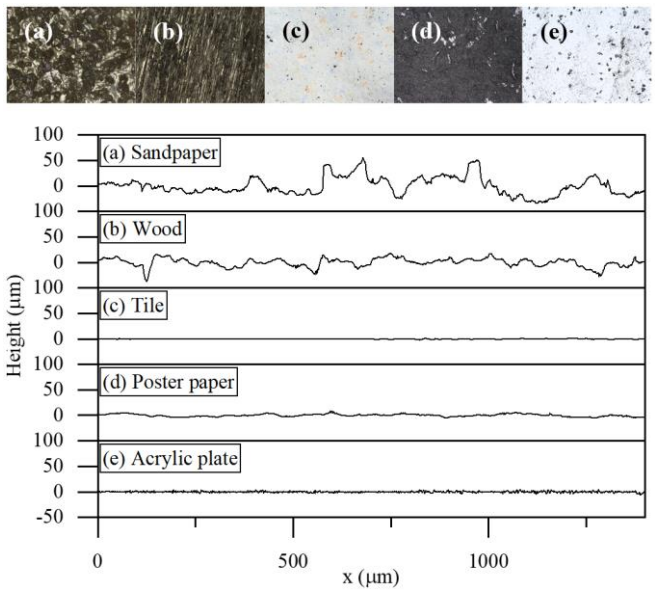

Figure 13 The optical microscope images and the surface roughness profiles of (a) a sandpaper, (b) a wooden plate, (c) a tile, (d) a poster paper, and (e) an acrylic plate used in the picking demonstration in Fig. 12.

IV. Conclusion

In this work, a gripper utilizing an SMP adhesive is designed, fabricated and tested. Picking and placing mechanisms are analyzed in particular to enable operating the gripper with a single hand. The dual SMP that is made of two different stiffness SMPs is designed to more evenly distribute stress at the adhesive interface, resulting in retarded contact failure and enhanced adhesion strength. Also, the SMP with release tip shows easy detachment in the experiment due to high stress concentration around the release tip. To optimize thermal conditions associated with the SMP adhesive gripper, a Peltier module is evaluated. Using Peltier modules for fast cooling is beneficial since reduced cooling time allows for more stable adhesive contact of the SMP against any disturbance including vibration during cooling. The numerical and experimental results show the successful pick-and-place capabilities of the SMP adhesive gripper and the feasibility of the potential use of it for wall climbing applications. For the future work, more quantitative study to verify the effect of preload and operation temperature on releasing force, adhesive contact failure and repeatability will be conducted.

REFERENCES

[1] A. Parness et al., "Gravity-independent Rock-climbing Robot and a Sample Acquisition Tool with Microspine Grippers," *J. of Field Robot.*, vol. 30, no. 6, pp. 897-915, Aug. 2013.

[2] H. Jiang et al., "A robotic device using gecko-inspired adhesives can grasp and manipulate large objects in microgravity," *Sci. Robot.*, vol. 2, no. 7, Jun. 2017.

[3] S. Ruggeri, G. Fontana, V. Basile, M. Valori and I. Fassi, "Micro-robotic Handling Solutions for PCB (re-)Manufacturing," Procedia Manuf., vol. 11, pp. 441-448, Jun. 2017.

[4] T. Stoyanov et al., "No More Heavy Lifting: Robotic Solutions to the Container Unloading Problem," *IEEE Robot. Autom. Mag.*, vol. 23, no. 4, pp. 94-106, Aug. 2016.

[5] A. Lourenço, F. Marques, R. Mendonça, E. Pinto and J. Barata, "On the design of the ROBO-PARNER Intra-factory Logistics Autonomous Robot," in *IEEE Int. Conf. on Syst., Man, Cybern.*, Budapest, 2018., pp. 2647-2652.

[6] C. Feng, Y. Xiao, A. Willette, W. McGee, and V. Kamat, "Towards autonomous robotic in-situ assembly on unstructured construction sites using monocular vision," in *Proc. of the 31th Int. Symp. on Autom. and Robot. in Construction*, 2014, pp. 163-170.

[7] J. Cecil*, D. Vasquez and D. Powell, "A review of gripping and manipulation techniques for micro-assembly applications," *Int. J. of Prod. Res.*, vol. 43, no. 4, pp. 819-828, Feb. 2005.

[8] H. Keum et al., "Microassembly of Heterogeneous Materials using Transfer Printing and Thermal Processing", *Scientific Rep.*, vol. 6, no. 1, 2016.

[9] Kim, "Micro-LEGO for MEMS", *Micromachines*, vol. 10, no. 4, p. 267, 2019.

[10] F. Y. Chen, "Gripping mechanisms for industrial robots," *Mechanism and Mach. Theory*, vol. 17, no. 5, pp. 299-311, Apr. 1982.

[11] K. Telegenov, Y. Tlegenov and A. Shintemirov, "A Low-Cost Open-Source 3-D-Printed Three-Finger Gripper Platform for Research and Educational Purposes," *IEEE Access*, vol. 3, pp. 638-647, May. 2015.

[12] K. H. Cho et al., "A robotic finger driven by twisted and coiled polymer actuator," in *Electroactive Polymer Actuators and Devices (EAPAD) 2016*, Vol. 9798. International Society for Optics and Photonics, 2016, pp. 97981J.

[13] D. Rus and M. T. Tolley, "Design, fabrication and control of soft robots," *Nature*, vol. 521, no. 7553, pp. 467-475, May. 2015.

[14] A. Parness, M. Frost, N. Thatte and J. P. King, "Gravity-independent mobility and drilling on natural rock using microspines," in *Robot. and Autom. (ICRA), 2012 IEEE Int. Conf. on*. IEEE, 2012, pp. 3437-3442.

[15] K. Nonaka, K. Sakai and J. Baillieul, "Open loop oscillatory control for electromagnetic actuated microgrippers.", *SICE 2004 Annual Conf.*, vol. 3, pp. 2285-2290, 2004.

[16] J. Shintake, S. Rosset, B. Schubert, D. Floreano and H. Shea, "Versatile Soft Grippers with Intrinsic Electroadhesion Based on Multifunctional Polymer Actuators," in *Adv. Mater.*, vol. 28, no. 2, pp. 231-238, 2016

[17] H. Zhang, J. Zhang, G. Zong, W. Wang and R. Liu, "Sky cleaner 3: A real pneumatic climbing robot for glass-wall cleaning," in *IEEE Robot. Autom. Mag.*, 2006, vol. 13, no. 1, pp. 32-41.

[18] T. Miyake, H. Ishihara and T. Tomino, "Vacuum-based wet adhesion system for wall climbing robots-lubricating action and seal action by the liquid," in *Robot. and Biomimetics, 2008. ROBIO 2008. IEEE International Conference on.* IEEE, 2009, pp. 1824-1829.

[19] S. Song, C. Majidi and M. Sitti, "Geckogripper: A soft, inflatable robotic gripper using gecko-inspired elastomer micro-fiber adhesives," in *Intelligent Robots and Systems (IROS 2014), 2014 IEEE/RSJ International Conference on.* IEEE, 2014. pp. 4624-4629.

[20] .S. Song, D. Drotlef, C. Majidi and M. Sitti, "Controllable load sharing for soft adhesive interfaces on three-dimensional surfaces", *Proc. of the Nat. Academy of Sci.*, vol. 114, no. 22, pp. E4344-E4353, 2017.

[21] J. Park, J. Eisenhaure and S. Kim, "Reversible Underwater Dry Adhesion of a Shape Memory Polymer", *Adv. Mater. Interfaces*, vol. 6, no. 3, p. 1801542, 2018. Available: 10.1002/admi.201801542.

[22] J. Eisenhaure and S. Kim, "High-strain shape memory polymers as practical dry adhesives," *Int. J. of Adhesion and Adhesives*, vol. 81, pp. 74-78, Mar. 2018.

[23] J. D. Eisenhaure et al., "The use of shape memory polymers for MEMS assembly," *J. of Microelectromechanical Syst.*, vol. 25, no. 1, pp. 69-77, Feb. 2016.

[24] J. Eisenhaure and S. Kim, "An internally heated shape memory polymer dry adhesive," *Polymers*, vol. 6, no. 8, pp. 2274-2286, Aug. 2014.

[25] J. D. Eisenhaure, T. Xie, S. Varghese and S. Kim, "Microstructured shape memory polymer surfaces with reversible dry adhesion," *ACS applied materials & interfaces*, vol. 5, no. 16, pp. 7714–7717, Aug. 2013.

[26] A. D. Astin, "Finger force capability: measurement and prediction using anthropometric and myoelectric measures," M.S. thesis, Dept. Ind. and Syst. Eng., Virginia Tech, Blacksburg, VA, 1999.

[27] H. Minsky and K. Turner, "Composite Microposts with High Dry Adhesion Strength", *ACS Appl. Mater. & Interfaces*, vol. 9, no. 21, pp. 18322-18327, 2017.